# A Multiview Microwave Imaging System for Two-Dimensional Penetrable Objects

Salvatore Caorsi, Gian L. Gragnani, *Member*, *IEEE*, and Matteo Pastorino, *Member*, *IEEE*

*Abstract*—**The microwave imaging system proposed in this paper is based on a multiview numerical solution to the integral equation of 2-D TM scattering. This solution is achieved by the moment method, and a pseudoinversion transformation is used to face ill-conditioning problems. An experimental setup is described that employs a scanning subsystem for measuring the values of the scattered electric field inside an observation domain located outside the investigation one (i.e., the area containing the cross sections of cylindrical dielectric scatters). Rotations of the investigation domain with respect to the scanning subsystem and the transmitting antenna allow a multiview imaging process.**

**The proposed imaging system does not require plane-wave illumination and does not use any first-order approximations; hence it may be used even in the case of strong scatterers. In addition, the off-line and once-and-for-all computation of the pseudoinverse matrix allows an inexpensive reconstruction in terms of computer resources. Some tests of the system were carried out, and the results are reported.**

## I. Introduction

In the last decade, the use of microwave imaging has drawn the attention of a notable number of researchers and industrialists. The need for designing and realizing adequate microwave imaging systems is felt particularly in the fields of geophysics [1], [2], aeronomic remote sensing [3], astronomy, and radio astronomy [4]. In addition, microwave imaging systems are becoming increasingly important for biomedical applications [5]–[7]. Moreover, in the industrial field, effective microwave imaging systems are required for numerous specific applications, among them robotic vision and nondestructive tests [8].

However, despite the large number of theoretical works and studies on inverse electromagnetic problems [9], more work needs to be done in order to realize adequate microwave imaging systems. Difficulties are encountered mainly in defining the interactions between microwaves and the materials commonly employed for imaging applications. The approximations related to ray propagation cannot be applied, because scattering phenomena, multiple paths, and other particular aspects must be taken into account. Furthermore, reconstruction algorithms utilize data that are often incomplete and noisy, as they are provided by imperfect scanning systems.

Moreover, most of the two- and three-dimensional wave transmission and reflection profile reconstruction methods use Born or Rytov approximations. These approximations are also utilized by imaging systems for biomedical and industrial applications of diffraction tomography [10]. All these methods are based on the relationship between image and projection transforms in the Fourier space. Nevertheless, there are severe limitations on the use of such methods, as already pointed out by many authors [11], [12]. In recent years, efforts have been devoted to developing microwave imaging systems that take fully into account electromagnetic scattering [13]–[15], even at the expense of an increase in both theoretical and practical difficulties.

This paper presents a prototype of an experimental system for microwave imaging purposes. The system utilizes a reconstruction algorithm based on a multiview solution to the problem of inverse electromagnetic scattering; such a solution has been obtained by using the moment method [16] and a pseudoinversion transformation [17]. In 1989, the authors proposed an approach to the reconstruction of the equivalent current density distribution [18] inside dielectric objects. The approach was based on inversion methodologies extensively studied in the last few years [13], [14], [19], [20] and made it possible to determine the locations and surface shapes of dielectric objects. Moreover, it was the basis for the reconstruction of the dielectric characteristics of two-dimensional objects [21]. A theoretical multiview version of that approach was also proposed [22].

In the present paper, a scanning and imaging system is proposed, and first evaluations of its reconstruction capabilities are made possible by preliminary measurements and inversion tests. The system exhibits interesting features that will make further development worthwhile. It does not require a plane-wave illumination of the investigation domain, and does not apply any first-order approximation; hence it can be potentially used even in the case of strong scatterers.

Another important feature of the system concerns the possibility of computing the pseudoinverse matrix off line and once and for all. As a result, the reconstruction process is not very heavy in terms of required computational resources.

Manuscript received July 14, 1990; revised November 27, 1990.

The authors are with the Department of Biophysical and Electronic Engineering, University of Genoa, Via all'Opera Pia, 11/a, 16145 Genova, Italy.

IEEE Log Number 9143001.

0018-9480/91/0500-0845$01.00 ©1991 IEEE

## II. Theoretical Background

The imaging system is based on a mathematical model for the inversion of the well-known formulation of two-dimensional electromagnetic scattering [23]. Let us assume that the region to be investigated has a complex permittivity

$$\tilde{\epsilon}(x,y) = \epsilon'(x,y) - j\epsilon''(x,y) \tag{1}$$

(which is the problem unknown) and is illuminated by an incident electric field $E^i$ polarized as a TM wave and propagating in the $y$ direction. The resulting scattered electric field, $E^s$, can be expressed in terms of both the complex conductivity and the total electric field, $E^t$, inside the investigation domain, as follows:

$$E^s(x,y) = k_0^2 \int_I [\tilde{\epsilon}(x',y') - 1] E^t(x',y') \cdot G(x,y/x',y')\, dx'\, dy' \tag{2}$$

where $G(x,y/x',y')$ is the two-dimensional Green function for free space [23].

Relation (2) holds at every point in space. In particular, we focus our attention on all the points $(x,y)$ belonging to a measurement domain $D$ (outside the investigation domain), where we measure the total electric field in order to evaluate the scattered electric field via the well-known relation

$$E^s = E^t - E^i. \tag{3}$$

We now rotate the region under test by an angle $\alpha$ with respect to the measurement setup. By repeating this procedure for $N$ angular positions $\alpha_1, \cdots, \alpha_N$ and according to (2), it is possible to write the $N$ integral equations

$$E^s(x,y,\alpha_n) = k_0^2 \int_I [\tilde{\epsilon}(x',y') - 1] E^t(x',y',\alpha_n) \cdot G(x,y,\alpha_n/x',y')\, dx'\, dy, \qquad n = 1, \cdots, N. \tag{4}$$

The equations allow one to image the scatterers under test by using multiview information. It is worth noting that each equation in relation (4) is a nonlinear one, since it includes the product of the complex permittivity by the total electric field, both of which are unknown quantities. Although the direct employment of this nonlinear formulation has been suggested in previous works [24], [25], it appears more convenient, owing to the difficulties related to nonlinear algorithms, to subdivide the problem into two linear steps, following an appropriate procedure to take into account the equivalent current density inside a cylindrical investigation domain. As is well known, such a current density is expressed as

$$J(x',y') = j\omega\epsilon_0 [\tilde{\epsilon}(x',y') - 1] E^t(x',y'). \tag{5}$$

By rearranging relation (4) in the light of (5), we obtain

$$E^s(x,y,\alpha_n) = j\omega\mu_0 \int_I J(x',y',\alpha_n) G(x,y/x',y')\, dx'\, dy', \qquad n = 1, \cdots, N \tag{6}$$

that is, a set of linear integral equations with the unknowns $J(x,y,\alpha_1) \cdots J(x,y,\alpha_N)$. The solutions to these equations allow one to derive the dielectric features of the scattering region by means of relation (5), also recalling that the total electric field inside the investigation domain can be expressed as

$$E^t(x,y) = E^i(x,y) + j\omega\mu_0 \cdot \int_I J(x',y') G(x,y/x',y')\, dx'\, dy'. \tag{7}$$

## III. Scanning and Imaging System Description

The previous section points out the necessity for solving equations (6) in order to develop an imaging system. To obtain numerical solutions to such equations, we adopt the moment method [16], so that each integral equation in (6) can be reduced to a linear algebraic system.

To this end, for each angular position $\alpha_n$ $(n = 1 \cdots N)$, the related equivalent current density is expanded into a sum of $M$ subsectional basis functions as follows:

$$J(x,y,\alpha_n) = \sum_m J^m_{\alpha_n}(x,y), \qquad n = 1, \cdots, N; \quad J^m_{\alpha_n}(x,y) = 0 \text{ outside the } m\text{th subsection}. \tag{8}$$

From a practical point of view, the use of such basis functions leads to a subdivision of the investigation domain into a regular square grid made up of square cells. For each angular position, the value of the equivalent current density inside each cell is taken to be constant.

We use $P$ Dirac deltas as testing functions for the scattered field inside the measurement domain; this simply leads to a measurement of the total field at $P$ points inside the measurement domain and to an evaluation of the scattered field via relation (3).

By applying the moment method, we obtain the following algebraic system:

$$[E^s] = [G][J] \tag{9}$$

where $[E^s] = [E^s_1 | E^s_2 | \cdots | E^s_N]$ is the $P \times N$ matrix whose columns are the $N$ arrays of the measures of the scattered electric field; $[G]$ is the $P \times M$ matrix derived from the discretization of the Green function; and $[J] = [J_1 | J_2 | \cdots | J_N]$ is the $M \times N$ matrix whose columns are the $N$ arrays of the equivalent current densities.

As is well known, the inverse problems related to the Fredholm equation of the first kind are ill posed. Likewise, the above-derived discretized problem is ill conditioned too, since the kernel properties of the integral equation are transferred into the matrix equation [26]. In particular, it is worth noting that the solution to a single-view, single-frequency inverse scattering problem may be nonunique, owing to the possible presence of so-called nonradiating sources [27]. Though the use of multiview measurements should improve the uniqueness of the solution [28], in order to overcome the difficulties arising from

ill conditioning, the solution to (9) is achieved via a pseudoinverse transformation [17], [29], which is a suitable tool for regularizing such problems. In this way, the matrix $[J]$ is given by

$$[J]=[G]^{+}[E^{s}] \tag{10}$$

where $[G]^{+}$ stands for the pseudoinverse matrix of $[G]$.

It should be stressed that, when using this approach, one can perform the evaluation of $[G]^{+}$ off line with respect to the imaging process. For a given measurement arrangement, this allows one to evaluate, once and for all, the pseudoinverse matrix, which can be stored in a computer memory and retrieved when needed.

Even though, in the past, some works [18], [30], have dealt with imaging based on the equivalent current, a more accurate image can be obtained by means of the dielectric features of the scattering region. In this case, a further step in the imaging process is required. To accomplish such dielectric reconstruction, we apply to (7) the same discretization procedure as previously used for the evaluation of $[J]$. The following algebraic relation can be written:

$$[E^{t}]=[E^{i}]+[G'][J] \tag{11}$$

where $[E^{t}]$ is the $M\times N$ matrix containing the array of the values of the total electric field inside the investigated region for each angular position; $[E^{i}]$ is the $M\times N$ matrix containing the values of the incident electric field inside the investigated region for each angular position (in practice, the incident field will be the same for each $\alpha_n$, so that $[E^{i}]$ will be made up of $N$ equal arrays); and $[G']$ is the $M\times M$ Green matrix for the scattering region.

From these relations, it is possible to deduce the total electric field inside the discretization domain, as it has been possible for the equivalent current density, for each angular position. From the values of the equivalent current and of the total electric field, one can derive, through relationship (5), the value of the dielectric permittivity of each cell for each angular position. It is worth noting that the region covered by a given cell varies for each angular position so that the system must take into account the relative positions of the discretization grid (which is fixed in space) and of the region to be investigated (which can be rotated). To this end, it is assumed that such a region is divided into pixels, and that each discretization cell covers more than one pixel. In general, the number of pixels can be arbitrary, although it is usually such as to provide standard images that can be $64\times 64$ up to $256\times 256$ pixels in size. The same pixel may belong to different discretization cells, depending on the angular position.

We use constant subsectional basis functions and Dirac's deltas as testing functions. This arrangement makes it possible to develop, in a straightforward way, a lookup table that, for any angular position, associates each pixel with the grid cells. This lookup table was conceived so as to obtain a trade-off between computer memory requirements and data access speed. The chosen cell numbering for the grid subdividing the investigation domain is shown in Fig. 1. If a given pixel belongs, for example, to the $m$th cell, after a rotation by an angle of 90° it will belong to the $(m+M/4)$th cell; after a rotation by an angle of 180° to the $(m+M/2)$th cell, and after a rotation by an angle of 270° to the $(m+3M/4)$th cell. Furthermore, we point out that, for any generic angular position $\alpha$, if the pixel $q_1$ on the coordinates $(x,y)$ belongs to the $h$th cell, then $q_2(x,-y)$ will belong to the $(h+M/4)$th cell, $q_3(-x,-y)$ to the $(h+M/2)$th cell, and $q_4(-x,y)$ to the $(h+3M/4)$th cell. On the basis of these considerations, only the first $M/4$ cells and the angular positions between 0 and 90° are considered in the lookup table, thus obtaining a notable saving in computer memory.

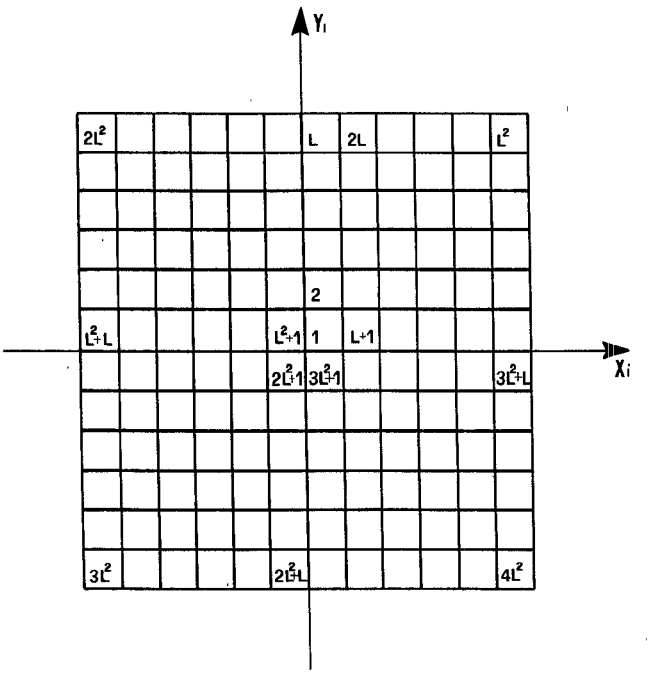


Fig. 1. Grid numbering (total number of cells = $4L^2$).

In summary, the proposed imaging system is subdivided into the following blocks: 1) an electromagnetic source producing an incident field; 2) a region to be investigated where unknown dielectric scatterers may be present and where the incident electric field must be known at each point; 3) a measurement system able to obtain the value of the total electric field by scanning a fixed region outside the region under investigation (at each point of this fixed region, the incident electric field must be known); and 4) a computer system implementing the inversion algorithm.

Moreover, it must be possible to rotate the region to be investigated by a certain angle to the electromagnetic source and to the scanning subsystem in order to collect multiview experimental data.

## IV. Experimental Setup Description

Fig. 2 shows our experimental setup. We use a transmitting aperture antenna whose large beam width makes it possible to illuminate the entire region under test. It

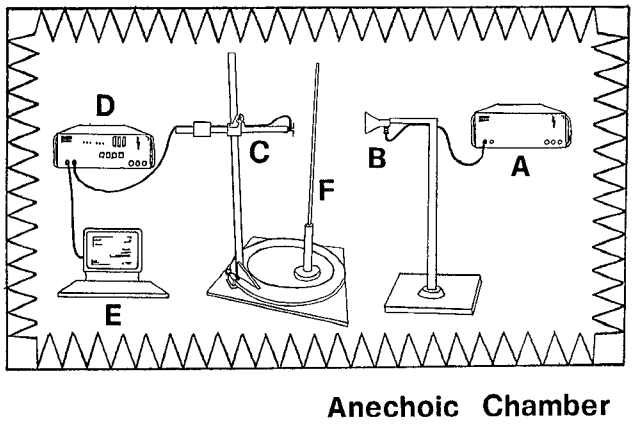


Fig. 2. Schematic representation of the experimental setup. $A$: signal source. $B$: transmitting antenna. $C$: scanning subsystem (rotating arm and receiving antenna). $D$: amplitude and phase meter. $E$: personal computer. $F$: long dielectric cylinder.

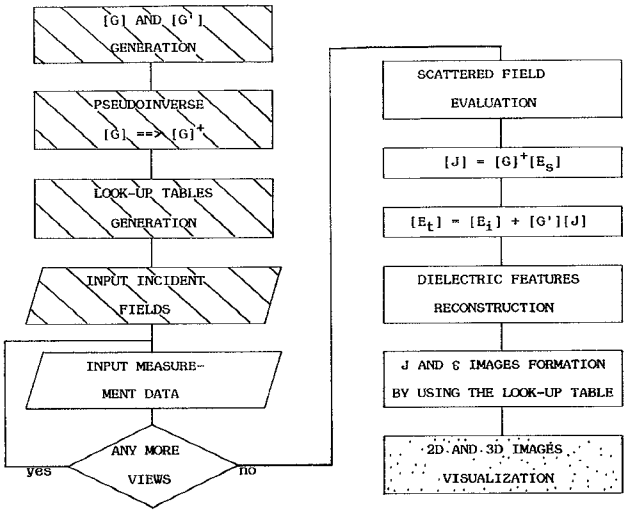


Fig. 3. Flowchart of the main computer processing steps. The hatched boxes indicate off-line procedures; the dotted boxes indicate graphic postprocessing steps.

should be noted that our approach does not require plane-wave illumination. It is well known that the need for such illumination is one of the most important drawbacks of other reconstruction systems.

The measurement subsystem is made up of a rotating arm whose position is controlled by a PC computer. A small electric dipole is used as a probe, and the scanning process is performed over an arc of a circumference whose center coincides with the center of the investigation domain.

The measured values of the total electric field are stored in the PC memory. In particular, the algorithm requires the values of the amplitude and phase of the electric field. To obtain these data, interferometric measurements between the probed signal and the reference signal are made through a chain made up of a bidirectional coupler, a phase shifter, and a precision attenuator. The collected data are then numerically treated by an HP 9000/825 minicomputer. Fig. 3 presents a flowchart of

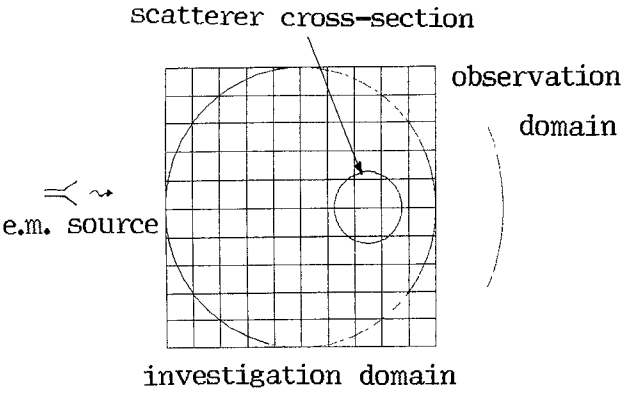


Fig. 4. Geometrical configurations of the investigation and observation domains. The greater circle indicates the actual area under test (i.e., the area involved in the multiview reconstruction process).

the main computer processing steps. We note that some of these steps are performed off line, while others can be regarded as postprocessing phases.

In particular, the on-line process consists in deducing the value of the scattered electric field from the value of the total electric field, after subtracting the value of the incident field; obtaining the product $[G]^+$ by $[E^s]$ to calculate the equivalent current; processing those data to calculate the dielectric permittivity; and constructing the final image by using the lookup table.

We note that the above on-line steps require limited computer resources, in that the most complex computations (i.e., the computation of the pseudoinverse $[G]^+$, the computation of $[G']$, and the preparation of the lookup table) can be performed off line once and for all.

## V. Experimental Examples and Discussion

The theoretical and numerical capabilities of the present imaging system have previously been discussed by the authors in other works, for both the single-view approach [21] and the multiview approach [22]. In this paper, we present some experimental results obtained by using the measurement setup described in Section IV.

In the experiments, we used a circular cylinder of polymethylmethacrylat, $12\lambda_0$ long, with a diameter equal to $d = \lambda_0/4$ and a relative dielectric permittivity equal to about 2.7. The operating frequency was chosen to be 3.0 GHz, and the cylinder was placed inside a $\lambda_0 \times \lambda_0$ square investigation domain partitioned into 100 square cells (each of which covered an 8 pixel $\times$ 8 pixel area). Through the superposition of the various views and the chosen pixel subdivision, one obtains an $80 \times 80$ image. Fig. 4 shows the geometrical configuration of the investigation area.

For each visual angle, we used eight measurement points only, arranged on a 45° arc of a circumference. On this arc, illustrated in the same figure, the points were equally spaced. It is worth noting that this arrangement (in particular, the low visual angles) was used to minimize the effects of the imperfect scanning subsystem, which exhibits a limited omnidirectionality feature.

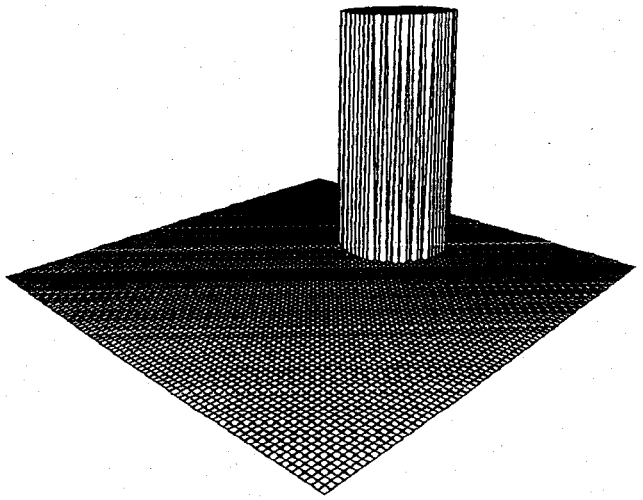

Fig. 5. A three-dimensional pictorial representation of the original relative dielectric permittivity distribution inside the investigation area.

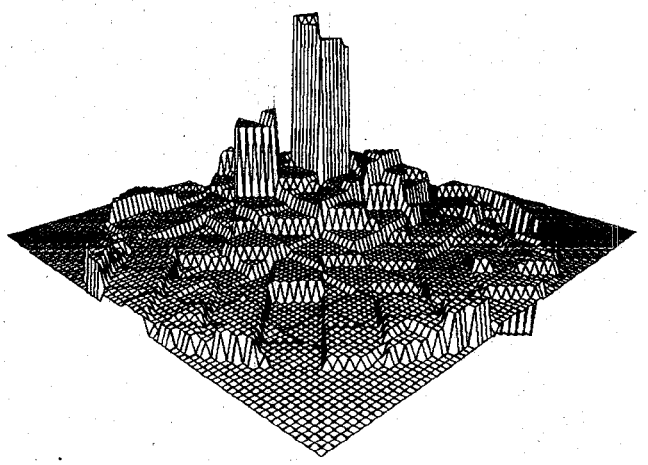

Fig. 7. A three-dimensional pictorial representation of the reconstructed relative dielectric permittivity inside the investigation domain, in the case of an eight-view imaging process. The maximum values are equal to 1.83, while the original value was 2.7.

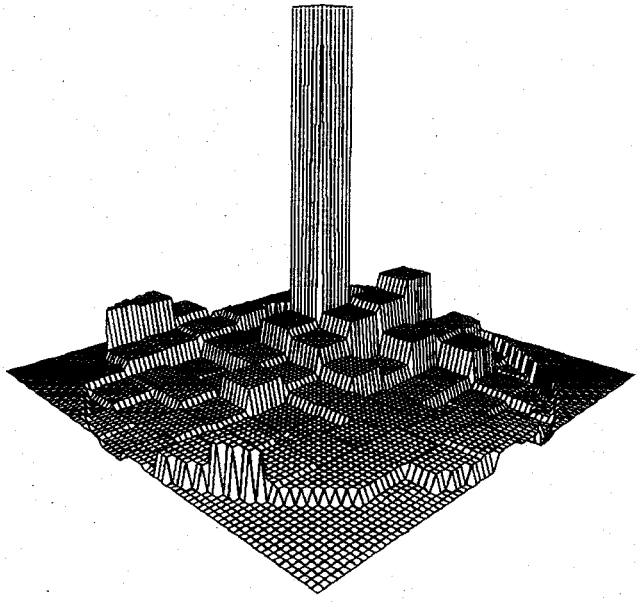

Fig. 6. A three-dimensional pictorial representation of the reconstructed relative dielectric permittivity inside the investigation domain, in the case of a four-view imaging process. The maximum values are equal to 2.31, while the original value was 2.7.

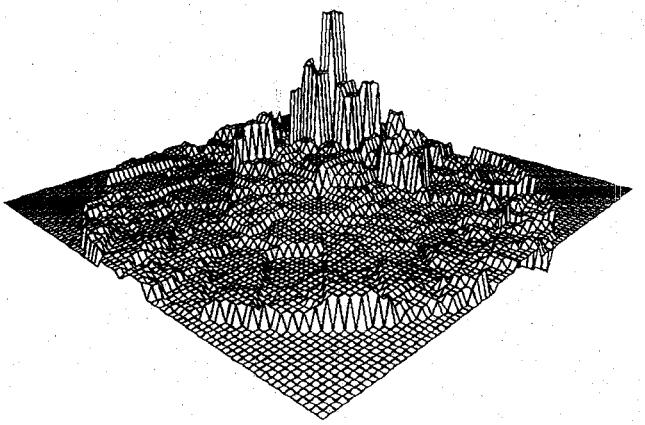

Fig. 8. A three-dimensional pictorial representation of the reconstructed relative dielectric permittivity inside the investigation domain, in the case of a 16-view imaging process. The maximum values are equal to 1.70, while the original value was 2.7.

TABLE I
DIELECTRIC PERMITTIVITY RECONSTRUCTION AND SCATTERER LOCALIZATION

| | 4 Views | 8 Views | 16 Views |
|---|---|---|---|
| Reconstructed permittivity | 2.30 | 1.83 | 1.70 |
| Localization error ($\lambda_0$ units) | 0.18 | 0.16 | 0.11 |

As mentioned in the numerical works cited above, the objective of the experiments was the reconstruction of the relative dielectric permittivity inside the investigation area. Over a wide range of values, this quantity was found to better shape the scattering objects, as compared with the equivalent current density.

Three examples were considered: the reconstruction process was performed in the cases of four, eight, and 16 views, corresponding to differences of 90°, 45°, and 22.5° in the related visual angles, respectively.

Fig. 5 shows a pictorial representation of the cylindrical scatterer (we note that the scale is not the same as in the following three figures), and pictorial representations of the results are presented in Figs. 6, 7, and 8. Table I gives the values of the reconstructed dielectric permittivity and the percentage errors on the localization of the cylinder; such errors refer to the distance from the center of the reconstructed area with maximum permittivity to the original center of the cylindrical scatterer. As can be deduced from the images and the values given in the table, the results are satisfactory for each case considered, in that the cylinder was localized with a maximum deviation of $0.18\lambda_0$, and the value of the dielectric reconstruction are in agreement with those reached by simulations for very low S/N ratios (as in the experiments). The results of such simulations allow one to predict that the present

microwave imaging system, by using multiple views, could achieve a more accurate shaping and a more precise localization of the scatterer, at the expense of a slightly lower dielectric reconstruction value. As far as the shaping of the cylinder is concerned, it turned out to be less accurate than that obtained by numerical simulations, perhaps as a consequence of the reduced visual angles utilized in the experiments and the fact that the source employed was not exactly TM; however, the experimental shaping can be considered acceptable, especially in the case of 16 views.

## VI. Conclusions

In this paper, we have presented an experimental microwave imaging system. From a theoretical standpoint, the imaging process is based on a multiview numerical solution to the integral equation of inverse electromagnetic scattering; such a solution has been obtained by using the moment method and a pseudoinverse transformation.

The proposed system does not require plane-wave illumination and could be used even for strong dielectric scatterers, as it is not based on Born or Rytov approximations.

An experimental setup has been described which allows one to record multiview data. The setup includes a scanning subsystem, so that the electric field scattered by a dielectric object (whose cross section is contained in the investigation area) can be measured at points located in an observation domain. The off-line computation of the pseudoinverse matrix allows a computationally inexpensive reconstruction of the dielectric characteristics of the investigation area.

Preliminary tests of the system were performed to achieve the dielectric reconstruction of a long cylinder illuminated by a source approximating a TM wave. Results prove that the system allows quite an accurate localization of the cross section of the scatterer inside the investigation area, as well as an approximate dielectric reconstruction. Although the results were obtained by using an imperfect experimental setup and low visual angles, they seem very promising for further developments in the area of microwave imaging. In the near future, the authors will perform a more complete set of experiments, in particular considering objects large in terms of $\lambda_0$ and with inhomogeneous dielectric permittivities.

## References


[1] A. J. Devaney, "Geophysical diffraction tomography," *IEEE Trans. Geosci. Remote Sensing*, vol. GE-22, pp. 3–13, 1984.

[2] A. Witten and J. E. Molyneux, "Geophysical imaging with arbitrary source illumination," *IEEE Trans. Geosci. Remote Sensing*, vol. 26, pp. 409–419, 1988.

[3] A. Deepak, *Inversion Methods in Atmospheric Remote Sensing*. New York: Academic, 1977.

[4] C. van Schooneveld, *Image Formation from Coherence Functions in Astronomy*. Dordrecht: D. Reidel, 1979.

[5] C. Pichot, L. Jofre, G. Peronnet, and J. C. Bolomey, "Active microwave imaging of inhomogeneous bodies," *IEEE Trans. Antennas Propagat.*, vol. AP-33, pp. 416–425, 1985.

[6] T. C. Guo, W. W. Guo, and L. E. Larsen, "A local study of water-immersed microwave antenna array for medical imagery," *IEEE Trans. Microwave Theory Tech.*, vol. MTT-32, pp. 844–854, 1984.

[7] T. C. Guo, W. W. Guo, and L. E. Larsen, "Recent development in microwave medical imaging—Phase and amplitude conjugations and the inverse scattering theorem," in *Medical Applications of Microwave Imaging*, L. E. Larsen and J. H. Jacobi, Eds. New York: IEEE Press, 1986, pp. 167–183.

[8] J. C. Bolomey, "Recent European developments in active microwave imaging for industrial, scientific, and medical applications," *IEEE Trans. Microwave Theory Tech.*, vol. 37, pp. 2109–2117, 1989.

[9] W. M. Boerner *et al.*, *Inverse Methods in Electromagnetic Imaging*, parts 1 and 2. Dordrecht: D. Reidel, 1985.

[10] A. J. Devaney, "Reconstructive tomography with diffracting wavefields," *Inverse Problems*, vol. 2, pp. 161–183, 1986.

[11] M. Slaney, A. C. Kak, and L. E. Larsen, "Limitation of imaging with first-order diffraction tomography," *IEEE Trans. Microwave Theory Tech.*, vol. MTT-32, pp. 860–873, 1984.

[12] J. C. Bolomey, C. Pichot, and G. Gaboriaud, "Critical and prospective analysis of reconstruction algorithms devoted to a planar microwave camera for biomedical applications," in *Proc. URSI Int. Symp. Electromagn. Theory* (Stockholm, Sweden), 1989, pp. 144–146.

[13] T. C. Guo and W. W. Guo, "Computation of electromagnetic wave scattering from an arbitrary three-dimensional inhomogeneous dielectric object," *IEEE Trans. Magn.*, vol. 25, pp. 2872–2874, 1989.

[14] M. M. Ney, A. M. Smith, and S. S. Stuchly, "A solution of electromagnetic imaging using pseudoinverse transformation," *IEEE Trans. Med. Imaging*, vol. MI-3, pp. 155–162, 1984

[15] D. K. Ghondgaonkar, O. P. Gandhi, and M. J. Hagmann, "Estimation of complex permittivities of three-dimensional inhomogeneous biological bodies," *IEEE Trans. Microwave Theory Tech.*, vol. MTT-31, pp. 442–446, 1983.

[16] R. F. Harrington, *Field Computation by Moment Method*. New York: Macmillan, 1968.

[17] R. Penrose, "A generalized inverse for matrices," *Proc. Cambridge Phil. Soc.*, vol. 51, pp. 406–413, 1955.

[18] S. Caorsi, G. L. Gragnani, and M. Pastorino, "Equivalent current density reconstruction for microwave imaging purposes," *IEEE Trans. Microwave Theory Tech.*, vol. 37, pp. 910–916, May 1989.

[19] T. C. Guo and W. W. Guo, "Three-dimensional dielectric imaging by inverse scattering with resolution unlimited by wavelength," in *Ann. Rep. Conf. Electrical Insulation and Dielectric Phenomena* (Leesburg, VA), 1989, pp. 65–74.

[20] T. C. Guo and W. W. Guo, "Dielectric imaging by microwave inverse scattering and a technique to stabilize matrix inversion," in *Proc. 2nd Int. Symp. Recent Advances in Microwave Technology*, pp. 33–38.

[21] S. Caorsi, G. L. Gragnani, and M. Pastorino, "Two-dimensional microwave imaging by a numerical inverse scattering solution," *IEEE Trans. Microwave Theory Tech.*, vol. 38, pp. 981–989, 1990.

[22] S. Caorsi, G. L. Gragnani, and M. Pastorino, "Image reconstruction by inverse-scattering solution for multiple microwave views," in *Proc. URSI Int. Symp. Electromagn. Theory* (Stockholm, Sweden), 1989, pp. 590–592.

[23] J. H. Richmond, "Scattering by a dielectric cylinder of arbitrary cross-section shape," *IEEE Trans. Antennas Propagat.*, vol. AP-13, pp. 334–341, 1965.

[24] S. A. Johnson, T. Yoon, and J. Ra, "Inverse scattering solutions of scalar Helmoltz wave equation by a multiple source moment method," *Electron. Lett.*, vol. 19, pp. 130–132, 1983.

[25] J. H. Rose, B. DeFacio, and M. Cheney, "Physical basis of three-dimensional inverse scattering for the plasma wave equation," *J. Opt. Soc. Amer. A*, vol. 2, pp. 1954–1957, 1985.

[26] T. Sarkar, D. D. Weiner, and V. K. Jain, "Some mathematical considerations in dealing with the inverse problem," *IEEE Trans. Antennas Propagat.*, vol. AP-29, pp. 373–379, 1981.

[27] A. J. Devaney and G. C. Sherman, "Nonuniqueness in inverse source and scattering problems," *IEEE Trans. Antennas Propagat.*, vol. AP-30, pp. 1034–1037, 1982.

[28] W. R. Stone, "A review and examination of results on uniqueness in inverse problems," *Radio Sci.*, vol. 22, pp. 1026–1030, 1987.

[29] M. M. Ney, "Method of moments as applied to electromagnetic problems," *IEEE Trans. Microwave Theory Tech.*, vol. MTT-33, pp. 972–980, 1985.
[30] J. C. Bolomey *et al.*, "Microwave diffraction tomography for biomedical applications," *IEEE Trans. Microwave Theory Tech.*, vol. MTT-30, pp. 1998–2000, 1982.

**Salvatore Caorsi** received the "laurea" degree in electronic engineering from the University of Genoa, Genoa, Italy, in 1973.

After graduation he remained at the university as a researcher, and since 1976 he has been Professor of Antennas and Propagation. In 1985 he also assumed the title of Professor of Fundamentals of Active Remote Sensing. He is with the Department of Biophysical and Electronic Engineering, where he is responsible for the Applied Electromagnetism Group and for the Research Center on the Interaction Between Electromagnetic Fields and Biological Systems (IEMBS). His activities deal primarily with applications of electromagnetic fields to telecommunications, artificial vision and remote sensing, biology, and medicine. In particular, he is working on research projects concerning microwave hyperthermia and radiometry in oncological therapy; numerical methods for solving electromagnetic problems; and inverse scattering and microwave imaging.

Prof. Caorsi is a member of the Associazione Elettrotecnica ed Elettronica Italiana (AEI), the European Bioelectromagnetics Association (EBEA) and the European Society for Hyperthermic Oncology (ESHO).

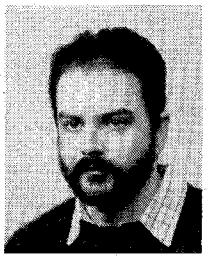

**Gian Luigi Gragnani** (M'89) received the "laurea" degree in electronic engineering from the University of Genoa, Genoa, Italy, in 1985.

In the same year, he joined the Applied Electromagnetism Group in the Department of Biophysical and Electronic Engineering. His primary interests are in electromagnetic scattering, both direct and inverse. In particular, he is involved with numerical methods for addressing electromagnetic problems, with microwave imaging, and with biomedical applications of electromagnetic fields, especially microwave hyperthermia. In addition, he is now doing research on electromagnetic compatibility.

Mr. Gragnani is a member of the Associazione Elettrotecnica ed Elettonica Italiana (AEI) and the European Bioelectromagnetics Association (EBEA).

**Matteo Pastorino** (M'90) is a Ph.D student of electronics and computer science in the Department of Biophysical and Electronic Engineering, University of Genoa, Genoa, Italy. He received the "laurea" degree in electronic engineering from the University of Genoa in 1987. Since that year, he has worked with the Applied Electromagnetism Group. His main research activities are in direct and inverse scattering, microwave imaging, wave propagation in the presence of nonlinear media, and numerical methods in electromagnetism. He is also working on research projects concerning biomedical applications of electromagnetic fields and microwave hyperthermia.

Mr. Pastorino is a member of the Associazione Elettrotecnica ed Elettronica Italiana (AEI) and the European Bioelectromagnetics Association (EBEA).